

# Identification of a state of persistent spin helix in a parallel magnetic field, and exploration of its transport properties

Yu. Ya. Tkach \*

*Kotel'nikov Institute of Radio Engineering and Electronics, Russian Academy of Sciences, Fryazino Branch, Fryazino, Moscow District 141190, Russia*



(Received 11 February 2022; accepted 29 March 2022; published 8 April 2022)

The tensors of conductivity and spin susceptibility of a two-dimensional electron gas (2DEG) with equal Rashba and Dresselhaus spin-orbit interaction constants [the persistent spin helix (PSH) state] in a parallel magnetic field are calculated. Applying a parallel magnetic field to the PSH state leads to the appearance of a saddle point in the spectrum and, accordingly, to a Van Hove singularity (VHS), whose amplitude increases indefinitely as the magnetic field strength ( $\mathbf{b}$ ) approaches to some critical value  $b_{cr}$ . The presence of a VHS in the density of states is an important factor determining the conductivity and spin susceptibility tensors. When only the lower spin subband is filled, the off-diagonal elements of the conductivity tensor are nonzero; that is, a Hall voltage arises due to the anisotropy of the Fermi surface and scattering. In the region where two spin subbands are filled, the diagonal and off-diagonal components of the spin susceptibility tensor are equal, and the off-diagonal terms of the conductivity tensor vanish. A sharp decrease in the conductivity and spin susceptibility at the beginning of the filling of the second spin subband, the ratio of the diagonal component of the spin susceptibility to the off-diagonal one, and also the number of critical points in the spectrum make it possible to establish the PSH 2DEG state.

DOI: [10.1103/PhysRevB.105.165409](https://doi.org/10.1103/PhysRevB.105.165409)

## I. INTRODUCTION

The state of persistent spin helix (PSH) in a two-dimensional electron gas (2DEG), although not very easy to obtain [1] has been attracting attention for a long time [2,3]. This is due to the understanding that the spin lifetime increases sharply when the Rashba and Dresselhaus constants coincide, as well as the stability of this state to a spin-independent potential, in particular, to the electron-electron Coulomb interaction [4]. The long spin lifetime gives reason to believe that a spin transistor in the spirit of Dutta and Das [5], as well as sources of polarized and spin current, can be created on the basis of the PSH state. Reviews of modern theoretical and experimental studies of the state of the PSH are given in the reviews [5,6].

It was shown [7] that when only the lower spin subband is filled in 2DEG with Rashba and Dresselhaus spin-orbit interactions (SOIs), logarithmic Van Hove singularities (VHSs) [8] (saddle points) appear in the one-particle density of states (DOS), the energy position of which can be controlled by a parallel magnetic field. At zero magnetic field, the singularity in the PSH state disappears [9]. The “amplitude” of VHS is determined by the curvature of the saddle point. The smaller the curvature, the more significant is the peak of the one-particle DOS, as well as the more significant are the measurable features in the conductivity and spin susceptibility in the Aronov-Lyand-Geller-Edelstein (ALGE) effect [10,11]. Here we can say that at a critical magnetic field, the

VHS becomes a higher-order singularity, which increases the possibility of their manifestations. Such singularities are currently being intensively studied [12,13]. A further increase in the magnetic field leads to the disappearance of this minimum and the saddle point. The DOS undergoes a jump at the beginning of the filling of the second spin subband. Usually, a jump in the DOS leads to a slight increase in the slope in the dependence of the conductivity on the Fermi level [14]. However, in the case of the PSH state, it is shown that this leads to a significant drop in the longitudinal conductivity and spin susceptibility.

The mutual influence of the SOI and a parallel magnetic field in a 2DEG system is of considerable interest, since a magnetic field allows one to manipulate the Fermi contour in a controllable manner, which is an effective tool for studying electron states and scattering processes. In the general case, when the magnetic field is oriented at an arbitrary angle with respect to the 2DEG plane, the spectrum and orbital motion of electrons undergoes a significant change [15]. The magnetic field in the plane is attractive, because a change in its intensity does not perturb the orbital wave functions, but changes the contour of the Fermi surface. This makes it possible to study the influence of the Fermi surface topology on an electron transport.

It was shown [16,17] that in a 2DEG with Rashba SOI and a parallel magnetic field the VHS leads to sharp dips in longitudinal conductivity and spin polarization during current flow, which is the ALGE effect. For elastic scattering of electrons by impurities with a short-range potential a method [16] was developed that allows one to solve this problem for arbitrary

\*utkach@gmail.com

Fermi contours at low temperatures in semiclassical approximation. It was shown that in this case the integral kinetic equation is a Fredholm integral equation with a degenerate kernel, therefore it reduces to an algebraic one and can be exactly solved. Due to the anisotropy of the Fermi surface, usually this is a difficult task [18].

When both the Rashba and Dresselhaus SOIs and a parallel magnetic field act simultaneously, there are four critical points in the energy spectrum: two minima and two saddle points, which in some directions can coincide or disappear with an increase in the magnetic field. The dispersion law for such a system was investigated in detail in Ref. [19]. In Ref. [9] the features of the conductivity tensor dependence on the magnetic field strength and the position of the Fermi level were studied. A technique allowing one to determine the constants of Rashba and Dresselhaus SOIs and the  $g$  factor from the position of VHS was also developed [9]. However, the PSH state in a parallel magnetic field has hardly been investigated. We will show that this state has a number of significant features, which enable one to identify this state measuring the conductivity tensor or spin susceptibility during the current flow (the ALGE effect).

## II. HAMILTONIAN AND ELECTRONIC STATES

In this section, we present the Hamiltonian and wave functions that will be used to calculate transport properties. The spectrum of 2DEG in a magnetic field oriented in a plane and with the spin-orbit interaction of Rashba and Dresselhaus was previously considered in [7,20]; the spectrum was studied in particular in the recent work [19]. We consider a two-dimensional electron gas without inversion symmetry, allowing a SOI that is linear in the electron wave vector. The most general form of linear coupling including both Rashba and Dresselhaus contributions has the following form [21,22]:

$$H = \frac{\mathbf{p}^2}{2m}\sigma_0 + \frac{\alpha}{\hbar}(p_x\sigma_y - p_y\sigma_x) + \frac{\beta}{\hbar}(p_x\sigma_x - p_y\sigma_y) - \frac{g^*}{2}\mu_B\mathbf{B}\sigma, \quad (1)$$

where  $\mathbf{p} = (p_x, p_y)$  is the electron momentum,  $p_x$  and  $p_y$  being its components along the [100] and [010] directions of a zinc-blende crystal, respectively,  $m$  is the effective mass,  $\alpha$  and  $\beta$  are the constants of Rashba and Dresselhaus SOIs,  $\sigma_x$  and  $\sigma_y$  are Pauli matrices,  $\mathbf{B} = B(\cos\zeta, \sin\zeta, 0)$  is a magnetic field strength, and  $\mu_B$  is the Bohr magneton.  $g^*$  is the effective Landé factor, which is assumed to be isotropic and independent of  $\mathbf{B}$ . The vector potential  $\mathbf{A}$  is written in the gauge  $\mathbf{A} = (0, 0, yB\cos\zeta - xB\sin\zeta)$ , at which the momentum in the plane  $(x, y)$  coincides with the generalized momentum. For the PSH state, the ratio of the Rashba and Dresselhaus SOI constants is equal to 1 ( $\alpha/\beta = 1$ ).

There are two types of eigenstates, which we will mark by the index  $\lambda = \pm$ . Their energies and wave functions have the form

$$\varepsilon_\lambda(\mathbf{q}) = q^2 + 2\lambda w(q'_y, \mathbf{b}) \quad (2)$$

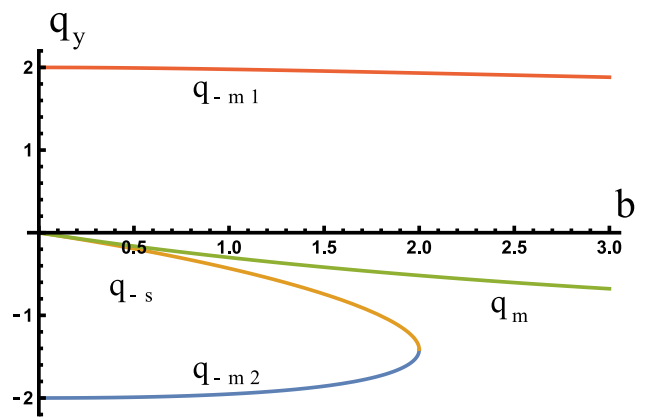


FIG. 1. Dependence of the coordinates  $q'_y$  of critical points on the magnetic field for its orientation  $\zeta' = \pi/4$ . Recall that for all critical points  $q_{x'} = 0$ .

and

$$\psi_{\mathbf{q}\lambda}(\mathbf{r}') = \frac{1}{\sqrt{2S^*}} \begin{pmatrix} 1 \\ i\lambda e^{i\varphi} \end{pmatrix} e^{i(q_{x'}x' + q_{y'}y')}. \quad (3)$$

Here and below, we used dimensionless quantities and passed to new variables:  $\varepsilon$  energy normalized to the characteristic energy of the Rashba SOI  $E_{so} = m\alpha^2/(2\hbar^2)$ ;  $\mathbf{q}$ —wave vector normalized to  $k_{so} = \alpha m/\hbar^2$ ;  $q_{x'} = (k_x + k_y)/(\sqrt{2}k_{so})$ ;  $q_{y'} = (k_y - k_x)/(\sqrt{2}k_{so})$ ;  $x' = (x + y)k_{so}/\sqrt{2}$ ;  $y' = (y - x)k_{so}/\sqrt{2}$ ;  $\mathbf{b} = g\mu_B\mathbf{B}\hbar^2/(2m\alpha^2)$ —dimensionless magnetic field,  $w(q_{y'}, \mathbf{b}) = \sqrt{q_{y'}^2 + 4bq_{y'}\cos[\zeta'] + b^2}$ ,  $b = |\mathbf{b}|$ ,  $\zeta' = \zeta - \pi/4$ ,  $S^*$ —sample area. This change of variables simplifies the study of the spectrum and leads to the fact that  $w(q_{y'}, \mathbf{b})$  does not depend on  $q_{x'}$ .

The phase  $\varphi(\mathbf{q})$  is defined by the following relations:

$$\sin\varphi = \frac{(q_{y'} + b_{x'})}{w(q_{y'}, \mathbf{b})}, \quad (4)$$

$$\cos\varphi = \frac{(-q_{y'} - b_{y'})}{w(q_{y'}, \mathbf{b})}. \quad (5)$$

Equating the derivatives of  $\varepsilon_\lambda(\mathbf{q})$  to zero, we obtain a system of two equations that determines the critical points of the spectrum:

$$q_{x'} = 0, \quad q_{y'}w(q_{y'}, \mathbf{b}) = -2\lambda(2q_{y'} + b\cos[\zeta']). \quad (6)$$

It can be seen from this system that the critical points are located on the  $q_{y'}$  axis and, according to the second equation, which must be squared to solve it, are the roots of an algebraic equation of the fourth degree. It is not difficult to solve it analytically, but the expressions for the roots are quite cumbersome, so we present a typical solution in Fig. 1 for a magnetic field with the direction  $\zeta' = \pi/4$ . Moreover, the squaring of this equation relieves our solution of dependence on  $\lambda$ , so it is easy to understand (see Fig. 2) that the critical points in the PSH state are two minima and a saddle point corresponding to the lower spin subband  $\varepsilon_{-m1,2}(q_{-m1,2})$  and  $\varepsilon_{-s}(q_{-s})$ , as well as the minimum corresponding to the appearance of the second spin subband  $\varepsilon_m(q_m)$ . An exception is the direction of the magnetic field corresponding to the angle

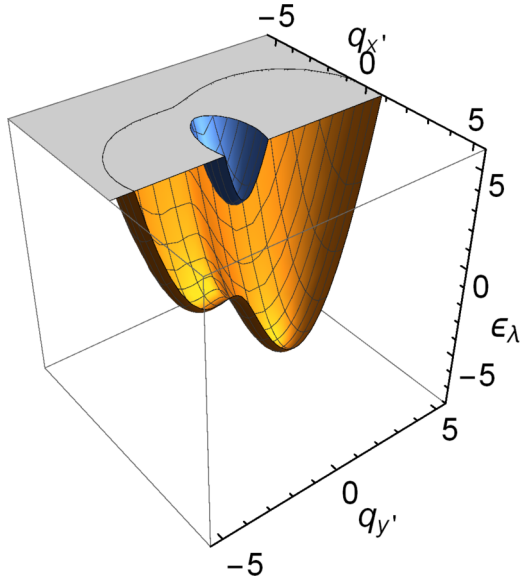


FIG. 2. A section of the energy landscape defined by Eq. (2) in the  $\mathbf{q}$  space. Here the blue and yellow surfaces correspond to  $\lambda = +$  and  $\lambda = -$ , respectively, with  $\zeta' = \pi/4$  and  $b = 1.8$ .

$\zeta' = 0$ . There is no manifestation of the saddle point for it because of the coincidence of energies  $\varepsilon_{-s} = \varepsilon_m$ . Also for the angle  $\zeta' = \pi/2$  both minima for the lower spin subband coincide in energy  $\varepsilon_{-m1} = \varepsilon_{-m2}$ , that is, for this orientation of the magnetic field in the density of states in the lower subband, we see one minimum and one saddle point, which merge at a critical magnetic field. For  $\pi \geq \zeta' \geq \pi/2$ , the graph of the roots differs from Fig. 1 by mirror reflection about the  $\mathbf{b}$  axis, that is, the roots for  $\zeta'$  and for  $\zeta' + \pi/2$  for fixed  $b$  differ by mirror reflection about the axis  $\mathbf{b}$ . For the coordinates of the critical points ( $q_{cr}$ ), it suffices to understand their location in the range of angles  $0 \leq \zeta' \leq \pi/2$ , since the following relation is additionally fulfilled:  $q_{cr}(\pi - \zeta') = q_{cr}(\pi + \zeta')$ .

For the direction of the magnetic field  $\zeta' = \pi/2$ , it is easy to obtain an analytical solution:

$$\begin{aligned} \varepsilon_{-m1, -m2}(\pm\sqrt{4 - b^2/4}) &= -4 - b^2/4, \\ \varepsilon_{-s,m}(0) &= \mp 2b. \end{aligned} \quad (7)$$

An important point is the appearance of a critical magnetic field ( $b_{cr}$ ), at which the minimum point and the saddle point merge. In this case, the amplitude of the VHS increases indefinitely (see Fig. 3). A further increase in the magnetic field leads to their disappearance (see Figs. 1 and 2).

To calculate the density of states  $N_s(\varepsilon)$ , the standard expression was used:

$$N_s(\varepsilon) = \frac{1}{\pi^2} \lim_{\Delta\varepsilon \rightarrow 0} \sum_{\lambda} \frac{S_{\lambda}(\varepsilon + \Delta\varepsilon) - S_{\lambda}(\varepsilon)}{\Delta\varepsilon}. \quad (8)$$

Here  $S_{\lambda}(\varepsilon)$  is the area in  $\mathbf{q}$  space that satisfies the inequality  $\varepsilon_{\lambda}(\mathbf{q}) \leq \varepsilon$ .

The dependence of the critical magnetic field, as well as the energy of critical points at this value of the field, on the angle of its orientation is shown in Fig. 4. Note that the dependence  $\varepsilon_{-m2}(\zeta')$  on it coincides with the dependence  $\varepsilon_{-s}(\zeta')$ . In fact, their equality is the equation that determines ( $b_{cr}$ ).

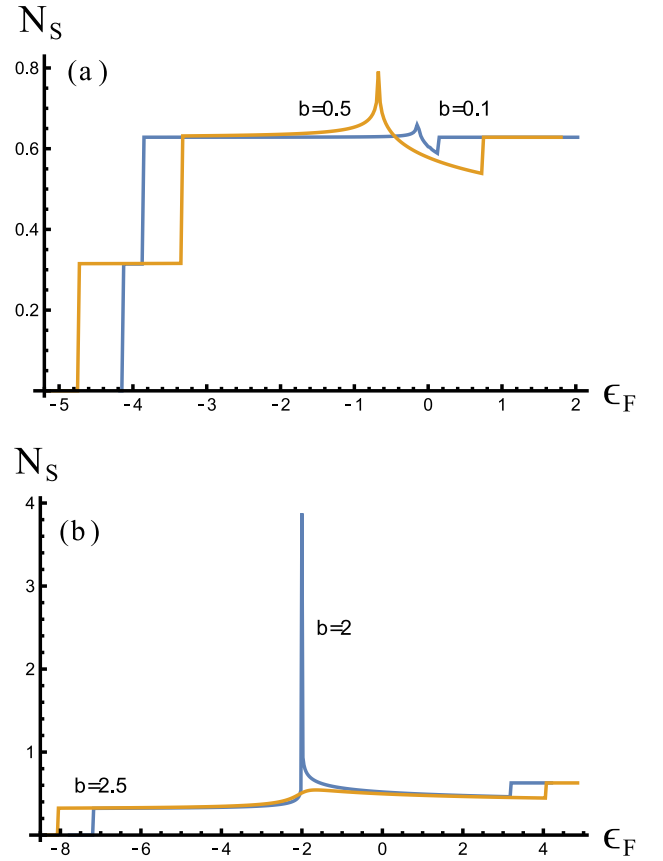


FIG. 3. Energy dependence of the density of states  $N_s(\varepsilon)$  for a set of magnetic fields oriented at an angle  $\zeta' = \pi/4$ .  $N_s$  is normalized to  $N_o = m/(\pi\hbar^2)$ .

### III. BOLTZMANN KINETIC EQUATION AND TRANSPORT PROPERTIES

Let us discuss the transport properties that arise when an electric field is applied. The electron current will be studied using the semiclassical Boltzmann equation. For a small uniform electric field  $\mathcal{E}$ , the distribution function  $f(\mathbf{k})$  is given by the Boltzmann equation [23]. Here and below, it is more convenient for us to return from the coordinates  $\mathbf{q}$  and  $\mathbf{r}'$  to the coordinates  $\mathbf{k}$  and  $\mathbf{r}$ , making them dimensionless in the same way as  $\mathbf{q}$  and  $\mathbf{r}'$ . The anisotropy of the dispersion law leads to

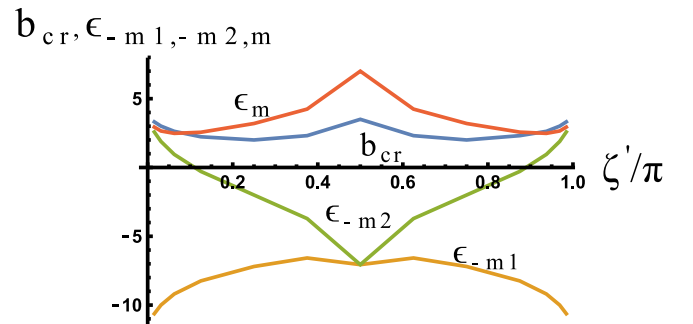


FIG. 4. Dependence of the critical magnetic field ( $b_{cr}$ ) and the energy of critical points at this value of the field on the angle of its orientation. (Recall that here all quantities are dimensionless.)

scattering anisotropy, therefore, the collision integral cannot be simplified by introducing the relaxation time. This problem has been discussed in detail in [18,24–27]. We managed to solve this rather complicated problem in [16] and additionally test it in [9,14]. As a test, in [9] we reproduced the results of [28,29], and in [28] the results coincide for the nonstandard dependence of the conductivity on the position of the Fermi level [ $G = \varepsilon_F + (\varepsilon_F)^2$ ] were obtained using both the Boltzmann kinetic equation and quantum computation using the Kubo formula.

We consider scattering by impurities with a short-range potential  $V(r) = V_0\delta(\mathbf{r})$ . The impurity concentration  $N$  is assumed to be low enough so that their potentials do not overlap and the process of scattering from different impurities is not correlated. Using the wave functions (3) and calculating the scattering probability in the Born approximation, we obtain the following equation for the nonequilibrium part of the distribution function  $\Delta f_\lambda(\mathbf{k})$ :

$$\sum_{\lambda'} \int \frac{d^2k'}{\pi} (1 + \lambda\lambda' \cos[\varphi(\mathbf{k}) - \varphi(\mathbf{k}')]) \delta[\varepsilon_\lambda(\mathbf{k}) - \varepsilon_{\lambda'}(\mathbf{k}')] \times [\Delta f_\lambda(\mathbf{k}) - \Delta f_{\lambda'}(\mathbf{k}')] = \frac{e\mathcal{E}\mathbf{v}_\lambda(\mathbf{k})}{R} \frac{\partial f_0}{\partial \varepsilon}, \quad (9)$$

where dimensionless quantities are used. The electric field  $\mathcal{E}$  is normalized to  $E_{so}k_{so}/e$ , the group velocity is  $\mathbf{v}_\lambda = \nabla_{\mathbf{k}}\varepsilon_\lambda(\mathbf{k})$ ,  $f_0$  is the equilibrium distribution function, and  $R$  is the only numerical parameter that appears in this system:  $R = V_0^2 N/\alpha^2$ .

The solution of this equation is described in detail in [9,16]. Let us recall the key moments of obtaining the solution and the basic formulas for calculating the conductivity and spin susceptibility tensors for the ALGE effect.

Let us rewrite the nonequilibrium function in the following form  $\Delta f_\lambda(\mathbf{k})$ :

$$\Delta f_\lambda(\mathbf{k}) = \frac{e\mathcal{E}}{R} \mathcal{F}_\lambda(\mathbf{k}) \frac{\partial f_0}{\partial \varepsilon}. \quad (10)$$

$$\mathcal{F}_{\lambda,r}(\phi, \theta) = \frac{\mathcal{G}_{\lambda,r}(\phi, \theta) + \mathfrak{A}(\theta) + \lambda\mathfrak{B}(\theta) \cos[\varphi_{\lambda,r}(\phi)] + \lambda\mathfrak{C}(\theta) \sin[\varphi_{\lambda,r}(\phi)]}{A + \lambda B \cos[\varphi_{\lambda,r}(\phi)] + \lambda C \sin[\varphi_{\lambda,r}(\phi)]}. \quad (15)$$

The coefficients  $A$ ,  $B$ , and  $C$  can be directly calculated, since the electron dispersion law is known (2). However, the coefficients  $\mathfrak{A}$ ,  $\mathfrak{B}$ , and  $\mathfrak{C}$  are determined by integrals containing the unknown functions  $\mathcal{F}_{\lambda,r}(\phi, \theta)$ . To obtain a system of equations that will allow us to find the coefficients  $\mathfrak{A}$ ,  $\mathfrak{B}$ , and  $\mathfrak{C}$ , we will substitute the expression (15) into Eq. (11).

As a result, we obtain a system of linear algebraic equations for these coefficients. To find the conductivity and spin susceptibility tensors, it suffices to calculate with the electric field oriented in the  $x$  and  $y$  directions ( $\theta = 0$  and  $\theta = \pi/2$ ). It should be taken into account that the determinants of the obtained systems are equal to zero, however, as well as additional determinants. This indicates the compatibility of the obtained systems and the lack of equations for determining the required coefficients ( $\mathfrak{A}$ ,  $\mathfrak{B}$ , and  $\mathfrak{C}$ ). Therefore, one of the equations in each resulting system is replaced by the electrical neutrality equation. Now we make sure that the determinant of the obtained systems for the orientations of

The function  $\mathcal{F}_\lambda(\mathbf{k})$  introduced by us is determined by an equation that can be easily obtained in the case of zero temperature by integrating modulo  $\mathbf{k}$  in Eq. (9). In this case, integration is performed over Fermi contours. Since in some cases the contours have complex shapes,  $k(\phi)$  is a multivalued function of  $\phi$ , so we are forced to divide the contours into parts for which  $k(\phi)$  becomes a single-valued function. Each part can be marked with an index  $r$ , which can vary from 1 to 4 depending on the shape of the Fermi contour. With this in mind, we will add this index to the notation for the function of the integrals that define the Fermi contours. The function  $\mathcal{F}_{\lambda,r}(\mathbf{k})$  defined on the Fermi part of the contour  $k = k_{\lambda,r}(\phi)$  is defined by the following equation:

$$\sum_{\lambda',r'} \int \frac{d\phi'}{\pi} (1 + \lambda\lambda' \cos[\varphi_{\lambda,r}(\phi) - \varphi_{\lambda',r'}(\phi')]) M_{\lambda',r'}(\phi') \times [\mathcal{F}_{\lambda,r}(\phi, \theta) - \mathcal{F}_{\lambda',r'}(\phi', \theta)] = \mathcal{G}_{\lambda,r}(\phi, \theta), \quad (11)$$

where

$$M_{\lambda,r}(\phi) = \left[ k \left/ \frac{\partial \varepsilon_\lambda(\mathbf{k})}{\partial k} \right]_{k=k_{\lambda,r}(\phi)}, \quad (12)$$

$$\varphi_{\lambda,r}(\phi) = \varphi(\mathbf{k})|_{k=k_{\lambda,r}(\phi)}, \quad (13)$$

$$\mathcal{G}_{\lambda,r}(\phi, \theta) = \frac{v_\lambda(\mathbf{k}) \cos[\xi(\mathbf{k}) - \theta]}{R} \Big|_{k=k_{\lambda,r}(\phi)}. \quad (14)$$

Here  $\xi(\mathbf{k})$  is the angle between  $\mathbf{v}_{\lambda,r}(\phi)$  and the  $x$  axis, and  $\theta$  is the angle between  $\mathcal{E}$  and the  $x$  axis. Quantities  $M_{\lambda,r}(\phi)$ ,  $\varphi_{\lambda,r}(\phi)$ , and  $\mathcal{G}_{\lambda,r}(\phi, \theta)$  are defined on the corresponding Fermi contours. They are easy to calculate using Eq. (11).

Equation (11) is solved analytically, since it is a linear Fredholm equation with a degenerate kernel. Representing its kernel as the sum of the products of the functions  $\phi$  and  $\phi'$  (these functions are actually just sines and cosines), we arrive at the following form of the function:

the electric field  $\theta = 0$  and  $\theta = \pi/2$  is not equal to zero and solve them. We find the corresponding coefficients  $\mathfrak{A}$ ,  $\mathfrak{B}$ , and  $\mathfrak{C}$ , which we substitute into Eq. (15), thereby determining the nonequilibrium distribution of electrons for these orientations of the electric fields in the form (15). For more details on the procedure for solving the kinetic equation, see [9,16].

Using the expression for the distribution function (15), we find the dimensionless components of the conductivity tensor:

$$G_{xx} = \sum_{\lambda,r} \int \frac{d\phi}{2\pi} M_{\lambda,r}(\phi) v_{\lambda,r}(\phi) \cos[\xi_{\lambda,r}(\phi)] \mathcal{F}_{\lambda,r}(\phi, 0), \quad (16)$$

$$G_{yx} = \sum_{\lambda,r} \int \frac{d\phi}{2\pi} M_{\lambda,r}(\phi) v_{\lambda,r}(\phi) \sin[\xi_{\lambda,r}(\phi)] \mathcal{F}_{\lambda,r}(\phi, 0), \quad (17)$$

normalized to  $e^2/(\hbar R)$ . The conductivity tensor components  $G_{xy}$  and  $G_{yy}$  differ from  $G_{xx}$  and  $G_{yx}$  by replacing  $\mathcal{F}_{\lambda,r}(\phi, 0)$

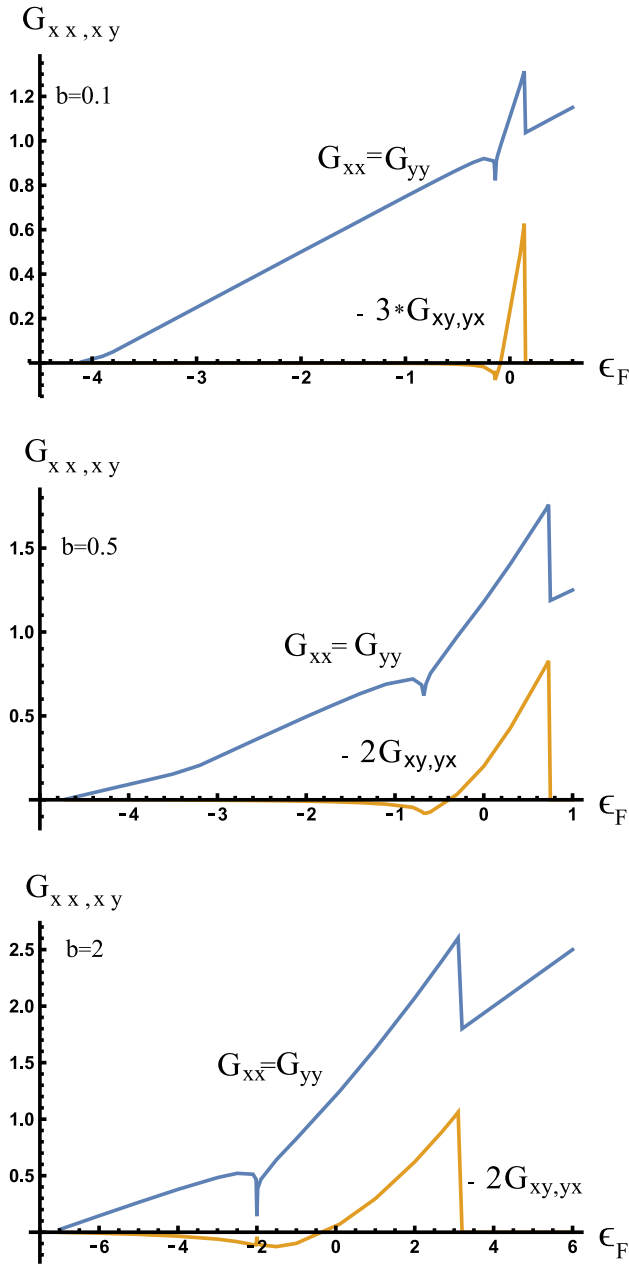


FIG. 5. Characteristic dependencies of the conductivity tensor on the position of the Fermi level for the orientation of the magnetic field  $\zeta = \pi/2$  or  $\zeta' = \pi/4$ .

with  $\mathcal{F}_{\lambda,r}(\phi, \pi/2)$ , respectively. In Fig. 5 we have presented the characteristic dependencies of the conductivity tensor on the position of the Fermi level for the orientation of the magnetic field  $\zeta' = \pi/4$  and  $b = 0.1; 0.5; 2$ , respectively.

In addition to the usual sharp decrease in conductivity near the VHS with increasing amplitude as the magnetic field approaches the critical ( $b_{cr} = 2$ ) [9,16], we unexpectedly see a sharp drop in conductivity when the Fermi level reaches the second spin subzones. This is due to a sharp decrease in the lifetime when the second recombination channel appears (Fig. 3). As the magnetic field increases, the off-diagonal term of the conductivity tensor and the amplitude of the peak  $G_{xy} =$

$G_{yx}$ , which arises when the second spin subband  $\varepsilon_F = \varepsilon_m$  appears, also increase.

The spin density induced by the electric field is given by the following expression:

$$S_i = \frac{\hbar}{2} \sum_{\lambda} \int \frac{d^2k}{4\pi^2} \langle \psi_{\lambda,\mathbf{k}}^{\dagger} | \sigma_i | \psi_{\lambda,\mathbf{k}} \rangle \Delta f_{\lambda}(\mathbf{k}), \quad (18)$$

where  $S_i$  is the projection of the spin density vector,  $i = (x, y, z)$ , and  $\sigma_i$  are the Pauli matrices. We define the spin susceptibility (often referred to as the Edelstein conductivity) as follows:

$$S_i = \sum_j \chi_{ij} \mathcal{E}_j. \quad (19)$$

Using Eqs. (3), (10), and (15), we find for the spin susceptibility,

$$\chi_{yx} = \sum_{\lambda,r} \lambda \int \frac{d\phi}{2\pi} M_{\lambda,r}(\phi) \cos[\xi_{\lambda,r}(\phi)] \mathcal{F}_{\lambda,r}(\phi, 0), \quad (20)$$

$$\chi_{xx} = - \sum_{\lambda,r} \lambda \int \frac{d\phi}{2\pi} M_{\lambda,r}(\phi) \sin[\xi_{\lambda,r}(\phi)] \mathcal{F}_{\lambda,r}(\phi, 0). \quad (21)$$

Here the Edelstein conductivity is normalized to  $e\hbar/(2\pi\alpha R)$ . The components of the spin susceptibility tensor  $\chi_{yy}$  and  $\chi_{xy}$  differ from  $\chi_{yx}$  and  $\chi_{xx}$  by replacing  $\mathcal{F}_{\lambda,r}(\phi, 0)$  with  $\mathcal{F}_{\lambda,r}(\phi, \pi/2)$ , respectively. There is no spin polarization in the  $z$  direction ( $S_z = 0$ ).

Characteristic dependencies of the components of the spin susceptibility tensor on the Fermi energy for the magnetic field orientation  $\zeta = \pi/2$  and  $b = 0.1; 0.5; 2$  are shown in Fig. 6. Similar to the conductivity tensor, the main features for the spin susceptibility arise when the Fermi level crosses the VHS and reaches the second spin subband. For the PSH state with a parallel magnetic field at  $\varepsilon_F > \varepsilon_m$ , the relations  $\chi_{yy} = -\chi_{xx} = 0.5$  and  $\chi_{xy} = -\chi_{yx} = 0.5$ , similar to the found relations for 2D electron gas without magnetic field [9].

#### IV. CONCLUSIONS

The inclusion of a parallel magnetic field for the PSH state leads to the appearance of a saddle point in the spectrum and, accordingly, to the Van Hove singularity, the amplitude of which increases indefinitely as the magnetic field approaches the critical  $b_{cr}$  (see Fig. 3). For almost all orientations of the magnetic field, there are three minima in the dispersion law (one of them when the second spin subband is reached) and one saddle point. All this is true for  $b < b_{cr}$ . The only exception is the direction of the magnetic field corresponding to the angle  $\zeta' = 0$ . There is no manifestation of a saddle point for it due to the coincidence of energies  $\varepsilon_{-s} = \varepsilon_m$ . Also, for the angle  $\zeta' = \pi/2$ , both minima for the lower spin subband coincide in energy  $\varepsilon_{-m1} = \varepsilon_{-m2}$ , i.e., for such an orientation of the magnetic field, we see one minimum and one saddle point in the density of states in the lower subband, which merge at a critical magnetic field. For  $\pi \geq \zeta' \geq \pi/2$  the graph of the roots differs from Fig. 1 by mirror reflection about the  $\mathbf{b}$  axis, i.e., the roots for  $\zeta'$  and for  $\zeta' + \pi/2$  for a fixed  $b$  differ in mirror reflection about the  $\mathbf{b}$  axis. For the coordinates of the critical points ( $q_{cr}$ ), it suffices to understand their location

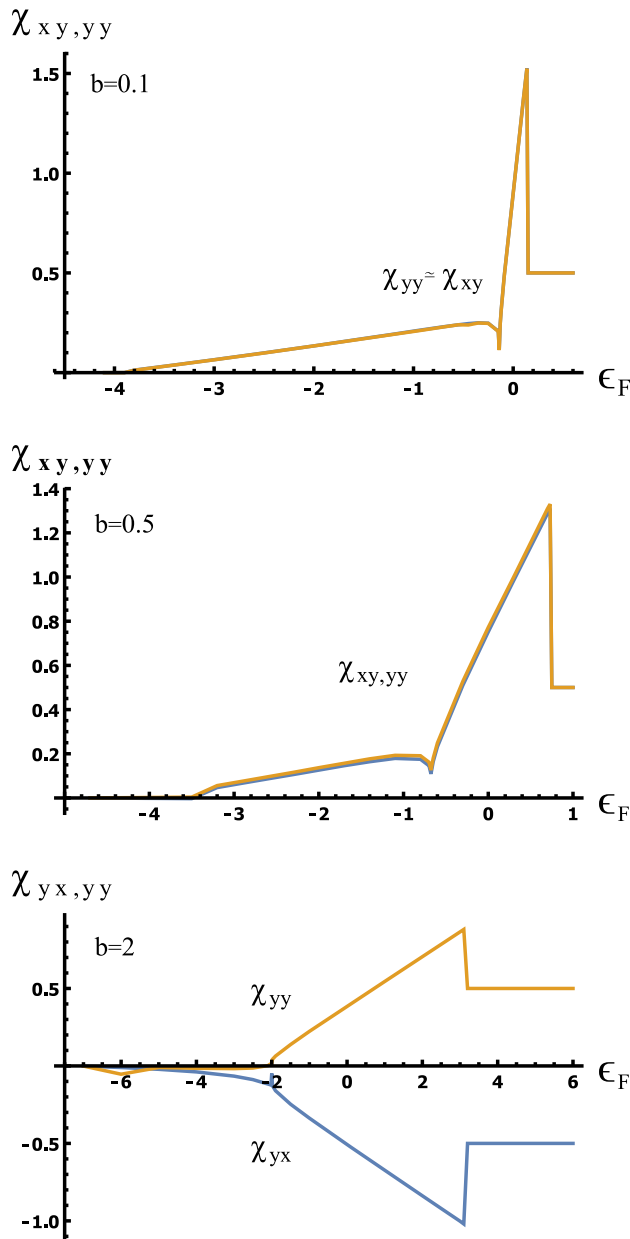


FIG. 6. Dependence of the components of the spin susceptibility tensor on the Fermi energy for the magnetic field orientation  $\zeta = \pi/2$  and  $b = 0.1; 0.5; 2$ , respectively.

in the range of angles  $0 \leq \zeta' \leq \pi/2$ , since the following relation is additionally fulfilled:  $q_{cr}(\pi - \zeta') = q_{cr}(\pi + \zeta')$ . For  $b > b_{cr}$ , the saddle point merges with the second minimum and disappears, that is, two minima remain in the dispersion law, one of which corresponds to the beginning of the spectrum, and the second to the appearance of the second spin subband (see Fig. 1).

The method developed to study anisotropic electron transport in 2DEG within the framework of the Boltzmann kinetic equation [16] is used to calculate the 2DEG conductivity and spin susceptibility tensors with equal Rashba and Dresselhaus SOIs in a wide range of parallel magnetic fields. This method makes it possible to accurately determine the nonequilibrium distribution function for scattering by impurities with a short-range potential at zero temperature, taking into account transitions both in one and in two different Fermi contours. An important factor determining the conductivity and spin susceptibility tensors is the presence of the VHS in the density of states, which arises due to the combined action of the SOIs and the parallel magnetic field. An unexpected thing is a sharp decrease in the components of the conductivity and spin susceptibility tensors upon reaching the Fermi level of the second spin subband (see Figs. 5 and 6).

All predicted effects can be observed. Difficulties can be associated with taking into account the many-particle effects [12,30], the insufficiently low temperature at which details are erased, and the influence of the fluctuation potential that arises with an increase in the concentration of scattering impurities. All these pitfalls for real observations are well known, and most of them are discussed in detail in [28]. One can agree with the statement in [28] that it is sufficient to use 2D structures with large SOI to observe the predicted features. In the same work, there are numerous references to experimental 2D systems that meet the required conditions. Note also that the inclusion of a parallel magnetic field due to the Zeeman effect makes it easier to observe the predicted features in transport phenomena.

#### ACKNOWLEDGMENTS

The author is grateful to V. A. Sablikov and B. S. Shchamkhalova for useful discussions and criticisms. This work was carried out in the framework of the state task and supported by the Russian Foundation for Basic Research, Project No. 20-02-00126.

[1] A. Sasaki, S. Nonaka, Y. Kynihashi, M. Konda, T. Bauernfeind, T. Dollinger, K. Richter, and J. Nitta, *Nat. Nanotechnol.* **9**, 703 (2014).  
 [2] N. S. Averkiev and L. E. Golub, *Phys. Rev. B* **60**, 15582 (1999).  
 [3] A. A. Kiselev and K. W. Kim, *Phys. Rev. B* **61**, 13115 (2000).  
 [4] B. A. Bernevig, J. Orenstein, and S.-C. Zhang, *Phys. Rev. Lett.* **97**, 236601 (2006).  
 [5] J. Schliemann, *Rev. Mod. Phys.* **89**, 011001 (2017).  
 [6] F. Passmann, S. Anghel, C. Ruppert, A. D. Bristow, A. V. Poshakinskiy, S. A. Tarasenko, and M. Betz, *Semicond. Sci. Technol.* **34**, 093002 (2019).  
 [7] Yu. Ya. Tkach, *JETP Lett.* **104**, 105 (2016).

[8] L. van Hove, *Phys. Rev.* **89**, 1189 (1953).  
 [9] Yu. Ya. Tkach, *Phys. Rev. B* **104**, 085413 (2021).  
 [10] A. G. Aronov and Yu. B. Lyanda-Geller, *JETP Lett.* **50**, 431 (1989).  
 [11] V. Edelstain, *Solid State Commun.* **73**, 233 (1990).  
 [12] Y.-T. Hsu, F. Wu, and S. Das Sarma, *Phys. Rev. B* **104**, 195134 (2021).  
 [13] A. Chandrasekaran and J. J. Betouras, *Phys. Rev. B* **105**, 075144 (2022).  
 [14] Yu. Ya. Tkach, *Phys. Status Solidi B* **258**, 2000553 (2021).  
 [15] R. Winkler, in *Spin-orbit Coupling Effects in Two-Dimensional Electron*, edited by J. Kuhn, T. Muller, A. Ruckenstein,

- F. Steiner, J. Trumper, and P. Wolffe, Springer Tracts in Modern Physics Vol. 191 (Springer, Berlin/Heidelberg, 2003).
- [16] V. A. Sablikov and Yu. Ya. Tkach, *Phys. Rev. B* **99**, 035436 (2019).
- [17] V. A. Sablikov and Yu. Ya. Tkach, *Semiconductors* **52**, 1581 (2018).
- [18] K. Vyborny, A. A. Kovalev, J. Sinova, and T. Jungwirth, *Phys. Rev. B* **79**, 045427 (2009).
- [19] I. V. Kozlov and Y. A. Kolesnichenko, *Phys. Rev. B* **99**, 085129 (2019).
- [20] E. P. Nakhmedov and O. Alekperov, *Eur. Phys. J. B* **85**, 298 (2012).
- [21] M. I. Dyakonov and V. Y. Kachorovski, *Phys. Tech. Poluprov.* **20**, 178 (1986).
- [22] P. Gambardella and I. Miron, *Philos. Trans. R. Soc. A* **369**, 3175 (2011).
- [23] I. Mertig, *Rep. Prog. Phys.* **62**, 237 (1999).
- [24] J. Schliemann and D. Loss, *Phys. Rev. B* **68**, 165311 (2003).
- [25] M. Trushin and J. Schliemann, *Phys. Rev. B* **75**, 155323 (2007).
- [26] P. Schwab and R. Raimondi, *Eur. Phys. J. B* **25**, 483 (2002).
- [27] O. Chalaev and D. Loss, *Phys. Rev. B* **77**, 115352 (2008).
- [28] V. Brosco, L. Benfatto, E. Cappelluti, and C. Grimaldi, *Phys. Rev. Lett.* **116**, 166602 (2016).
- [29] A. Johansson, J. Henk, and I. Mertig, *Phys. Rev. B* **93**, 195440 (2016).
- [30] Y. Tian, N. Ghassemi, and J. H. Ross, *Phys. Rev. B* **100**, 165149 (2019).